

Supplementary Material

Gypsum endolithic phototrophs under moderate climate (Southern Sicily): their diversity and pigment composition

Kateřina Němečková*, Jan Mareš, Lenka Procházková, Adam Culka, Filip Košek, Jacek Wierzechos, Linda Nedbalová, Jan Dudák, Veronika Tymlová, Jan Žemlička, Andreja Kust, Jan Zima Jr., Eva Nováková, and Jan Jehlička¹

* **Correspondence:** Corresponding Author: katerina.nemeckova@natur.cuni.cz

Table S1: Raman bands of the detected pigments.

Table S2: Table of samples used for metagenomics analysis, their lithology, characterization of endolithic colonization and relative abundance of endolithic phototrophs.

Figure S1: Micro-CT 3D reconstructions and selected slices illustrating the inner architecture and void space of gypsum fragments. Samples from Monte Perrera - MP1 (A – B) and MP2 (D – F); and from Monte Gibliscemi MG (G– I). The red and green frames in the 3D images show the position of the displayed slices.

Figure S1: Non-metric Multi-Dimensional Scaling (NMDS) analysis of the diversity among gypsum endolithic samples from two localities in Sicily. Samples from the studied localities are enclosed within convex hulls with centroids marked by asterisks (Siculiana Marina – black, full line, Santa Elisabetta – grey, dashed line). The analysis was based on Bray-Curtis distance matrix inferred from normalized abundances of the amplicon sequence variants (ASVs). The samples from Siculiana Marina exhibited greater overall diversity (they were also greater in number).

Figure S2: Non-metric Multi-Dimensional Scaling (NMDS) analysis of the diversity among gypsum endolithic samples from two different gypsum varieties. Samples from the studied substrates are enclosed within convex hulls with centroids marked by asterisks (selenite – black, full line, crystalline gypsum – grey, dashed line). The analysis was based on Bray-Curtis distance matrix inferred from normalized abundances of the amplicon sequence variants (ASVs). The samples from selenite exhibited greater overall diversity (but they were also significantly greater in number).

Figure S3: Non-metric Multi-Dimensional Scaling (NMDS) analysis of the diversity among gypsum endolithic samples from two differently coloured layers of colonization. Samples from the studied

endolithic layers are enclosed within convex hulls with centroids marked by asterisks (black zone – black, full line, green zone – grey, dashed line). The analysis was based on Bray-Curtis distance matrix inferred from normalized abundances of the amplicon sequence variants (ASVs). The samples from black layers exhibited greater overall diversity.

Site	Sample/ colour of colonisation	Organism	Identified pigment	Detected Raman bands
Siculiana Marina	1CF black	<i>Nostoc</i> sp.	scytonemin	1712 w, 1633 m, 1600 s , 1558 m, 1387 w, 1324 w, 1174 ms , 1098 mw, 1023 w, 755 w, 681 w
		<i>Gloeocapsa</i> sp.	gloeocapsin	1671 m, 1289 m, 480 mw
		<i>Gloeocapsopsis pleurocapsoides</i>	carotenoid	1516 vs , 1449 w, 1388 w, 1283 mw, 1189 mw, 1155 ms , 1004 m, 957 w
Monte Perrera site	S12 black	<i>Gloeocapsa compacta</i>	gloeocapsin	1668 s , 1571 s , 1424 ms , 1340 m, 1280 ms , 1190 m, 465 m, br
		<i>Nostoc</i> sp.	scytonemin	1711 w, 1633 m, 1598 s , 1555 m, 1381 mw, 1171 ms , 573 w, 436 w
		<i>Nostoc</i> sp.	carotenoid	1513 vs , 1283 w, 1193 m, 1155 s , 1003 m, 958 w
Monte Giblicemi	S14 orange	<i>Chlorophyta</i>	carotenoid	1517 s , 1447 w, 1389 w, 1274 w, 1191 ms , 1156 s , 1005 m, 964 w

Table S1: Raman bands of the detected pigments.

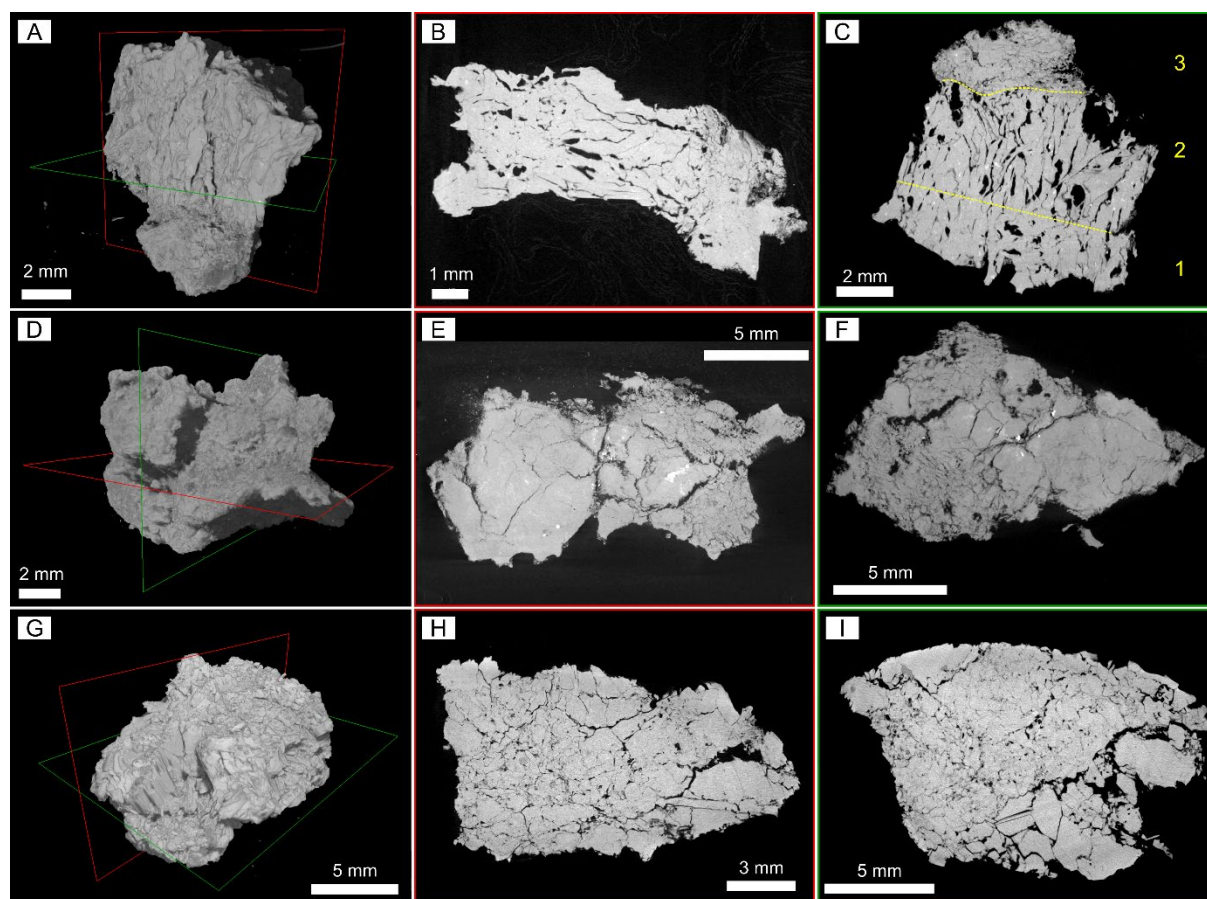


Figure S1: Micro-CT 3D reconstructions and selected slices illustrating the inner architecture and void space of gypsum fragments. Samples from Monte Perrera - MP1 (A – B) and MP2 (D – F); and from Monte Gibliscemi MG (G– I). The red and green frames in the 3D images show the position of the displayed slices.

Site	Lithology	Layer	Sample ID	Relative abundance		
				< 5 %	5-49 %	> 50 %
Siculiana Marina	Selenite	Green	1	<i>Nostoc</i> sp., <i>Microcoleus</i> sp., <i>Anathece</i> sp.	<i>Chroococcidiopsis</i> sp., <i>Chroococcus</i> sp., <i>Gloeocapsa</i> sp., orange-pigmented algae	-
			2	<i>Gloeocapsa novacekii</i> , <i>G. rupestris</i> , <i>Nostoc</i> sp., <i>Chroococcus</i> sp.	<i>Chroococcidiopsis</i> sp., <i>Gloeocapsa</i> sp.	-
			3	<i>Nostoc</i> sp. <i>G. rupestris</i>	<i>Gloeocapsa</i> sp.	<i>Chroococcidiopsis</i> sp.,
			4	<i>Chroococcus</i> , <i>G. Compacta</i> , <i>Nostoc</i> sp., <i>Anathece</i> sp., <i>Petalonema</i> sp.	<i>Gloeocapsa</i> sp., <i>G. rupestris</i>	<i>Chroococcidiopsis</i> sp.,
			5		<i>Chroococcidiopsis</i> sp., <i>G. rupestris</i> , <i>G. novacekii</i>	<i>Gloeocapsa</i> sp.
			6	<i>Chroococcus</i> sp., <i>G. compacta</i>	<i>Chroococcidiopsis</i> , <i>Gloeocapsa</i> sp., algae	-
		Black	7		<i>Chroococcidiopsis</i> sp., algae	<i>Nostoc</i> sp.
			8	<i>Gloeobacter violaceus</i> , <i>Nostoc</i> sp., <i>Chroococcidiopsis</i> sp., <i>G. novacekii</i>	, <i>Gloeocapsa</i> sp., <i>G. rupestris</i> , algae	<i>G. compacta</i>
			9			<i>Nostoc</i> sp.
			10		algae	
			11	<i>Chroococcidiopsis</i> sp.	<i>Nostoc</i> sp., <i>Gloeocapsa</i> sp.	<i>Petalonema</i> sp.
			12	<i>Petalonema</i> sp., algae	<i>Gloeocapsa</i> sp.	<i>Nostoc</i> sp.
			13	<i>G. novacekii</i> , <i>Nostoc</i>	<i>G. pleurocapsoides</i> , <i>G. rupestris</i> , <i>Gloeocapsa</i> sp. (bezbarvá)	<i>G. compacta</i>
	White crystalline	Green	14	<i>Gloeocapsa</i> sp., <i>G. compacta</i> , <i>Nostoc</i> sp.	-	<i>Chroococcidiopsis</i> sp.,
		Black	15	<i>Petalonema</i> sp., <i>Chroococcidiopsis</i> sp., <i>Nostoc</i> sp.	<i>Gloeocapsa</i> sp., <i>G. compacta</i> , <i>G. biformis</i> , <i>G. rupestris</i> , <i>Gloeobacter violaceus</i>	-
		Green	16	<i>Gloeocapsa</i> sp., <i>Nostoc</i>		<i>Chroococcidiopsis</i> sp.,
		Black	17	<i>Gloeocapsa</i> sp., <i>G. novacekii</i> , <i>Nostoc</i> sp.	<i>Chroococcidiopsis</i> sp., <i>Gloeobacter violaceus</i> , <i>G. rupestris</i> , <i>G. compacta</i> , <i>G. biformis</i> , <i>Petalonema</i> sp.	-
		Green	18		<i>Nostoc</i> sp.	<i>Chroococcidiopsis</i> sp.,
		Black	19	<i>Petalonema</i> sp., <i>Chroococcus</i> sp., <i>G. novacekii</i> ,	<i>Chroococcidiopsis</i> sp., <i>Nostoc</i> sp., <i>G. compacta</i>	-
		Black	20	<i>Nostoc</i> sp., <i>G. novacekii</i>	<i>Gloeocapsa</i> sp., <i>G. compacta</i> , <i>G. rupestris</i> , <i>Chroococcidiopsis</i> sp.	-
Santa Elisabetta	Selenite	green	21	<i>Petalonema</i> sp., algae	<i>Gloeocapsa</i> sp., algae	<i>Chroococcidiopsis</i> sp.,
		black	22		<i>Gloeocapsa</i> sp., <i>Nostoc</i> sp., <i>G. biformis</i> , algae	-
		black	23	<i>Chroococcidiopsis</i> sp., algae	<i>G. rupestris</i>	<i>Gloeobacter violaceus</i>
		black	24	Orange-pigmented algae	<i>Nostoc</i> sp.	<i>Chroococcidiopsis</i> sp.,
		green	25		<i>Chroococcidiopsis</i> sp., <i>Nostoc</i> sp.	<i>Gloeocapsa</i> sp.
		green	26	<i>Chroococcidiopsis</i> sp., algae	-	<i>Gloeobacter violaceus</i>
		black	27		<i>Nostoc</i> sp., <i>Chroococcidiopsis</i> sp., algae	-

Table S2: Table of samples used for metagenomics analysis, their lithology, characterization of endolithic colonization and relative abundance of endolithic phototrophs.

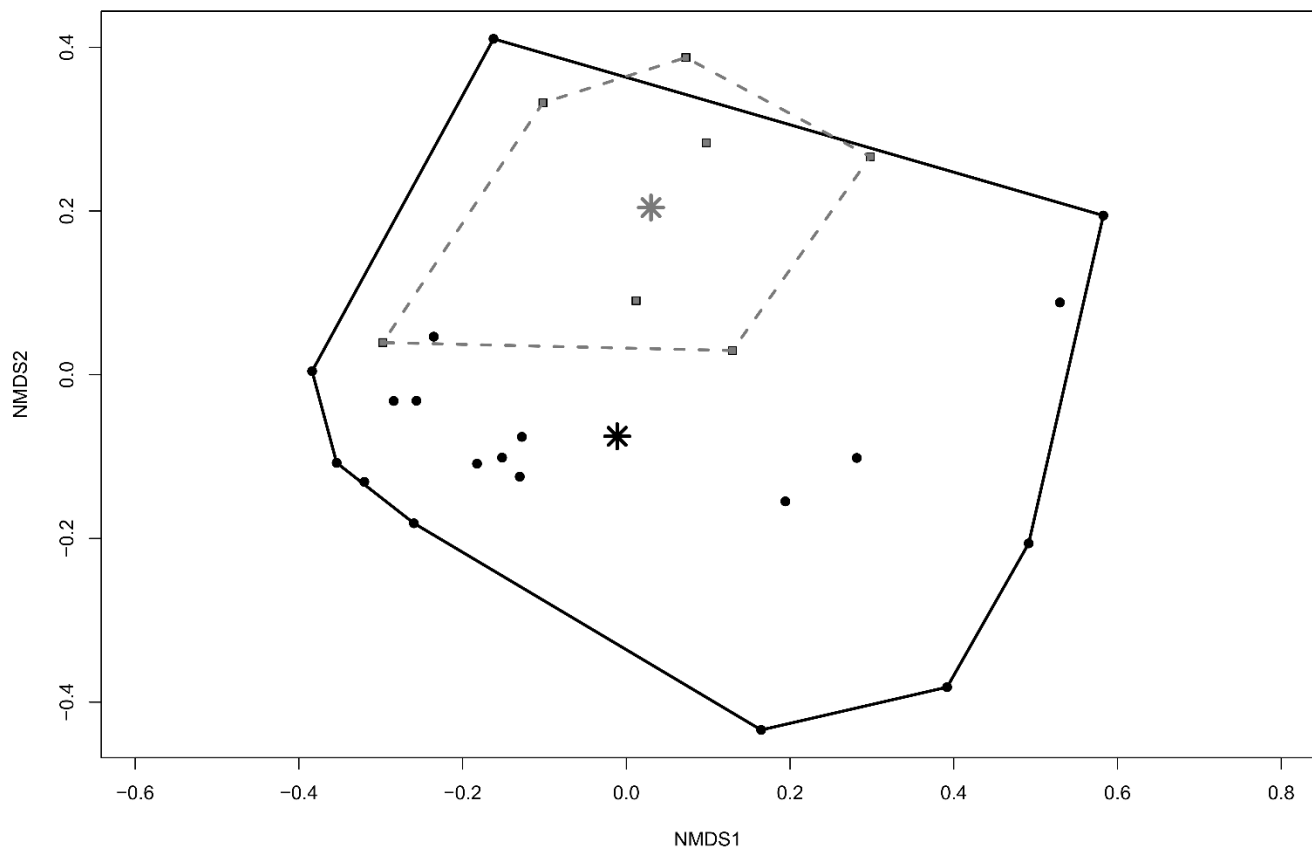


Figure S2: Non-metric Multi-Dimensional Scaling (NMDS) analysis of the diversity among gypsum endolithic samples from two localities in Sicily. Samples from the studied localities are enclosed within convex hulls with centroids marked by asterisks (Siculiana Marina – black, full line, Santa Elisabetta – grey, dashed line). The analysis was based on Bray-Curtis distance matrix inferred from normalized abundances of the amplicon sequence variants (ASVs). The samples from Siculiana Marina exhibited greater overall diversity (they were also greater in number).

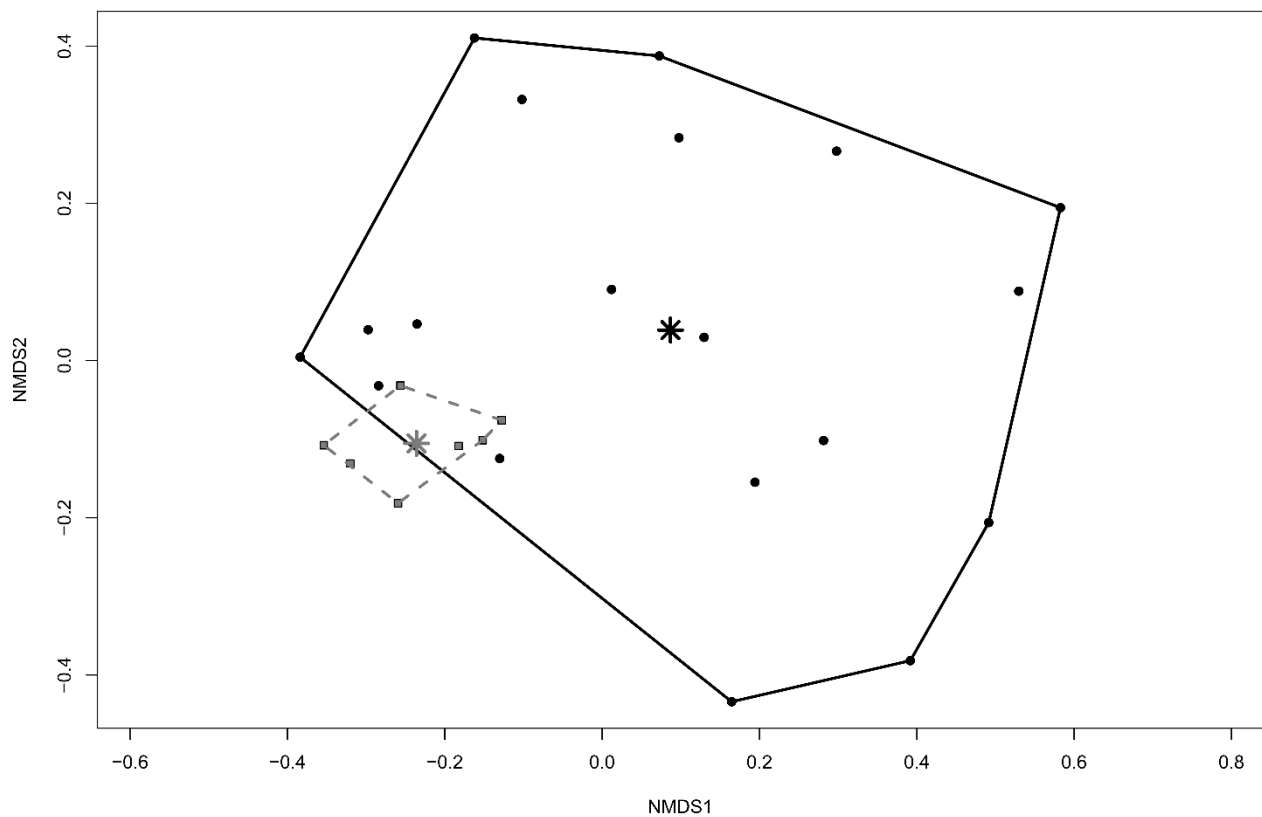


Figure S3: Non-metric Multi-Dimensional Scaling (NMDS) analysis of the diversity among gypsum endolithic samples from two different gypsum varieties. Samples from the studied substrates are enclosed within convex hulls with centroids marked by asterisks (selenite – black, full line, crystalline gypsum – grey, dashed line). The analysis was based on Bray-Curtis distance matrix inferred from normalized abundances of the amplicon sequence variants (ASVs). The samples from selenite exhibited greater overall diversity (but they were also significantly greater in number).

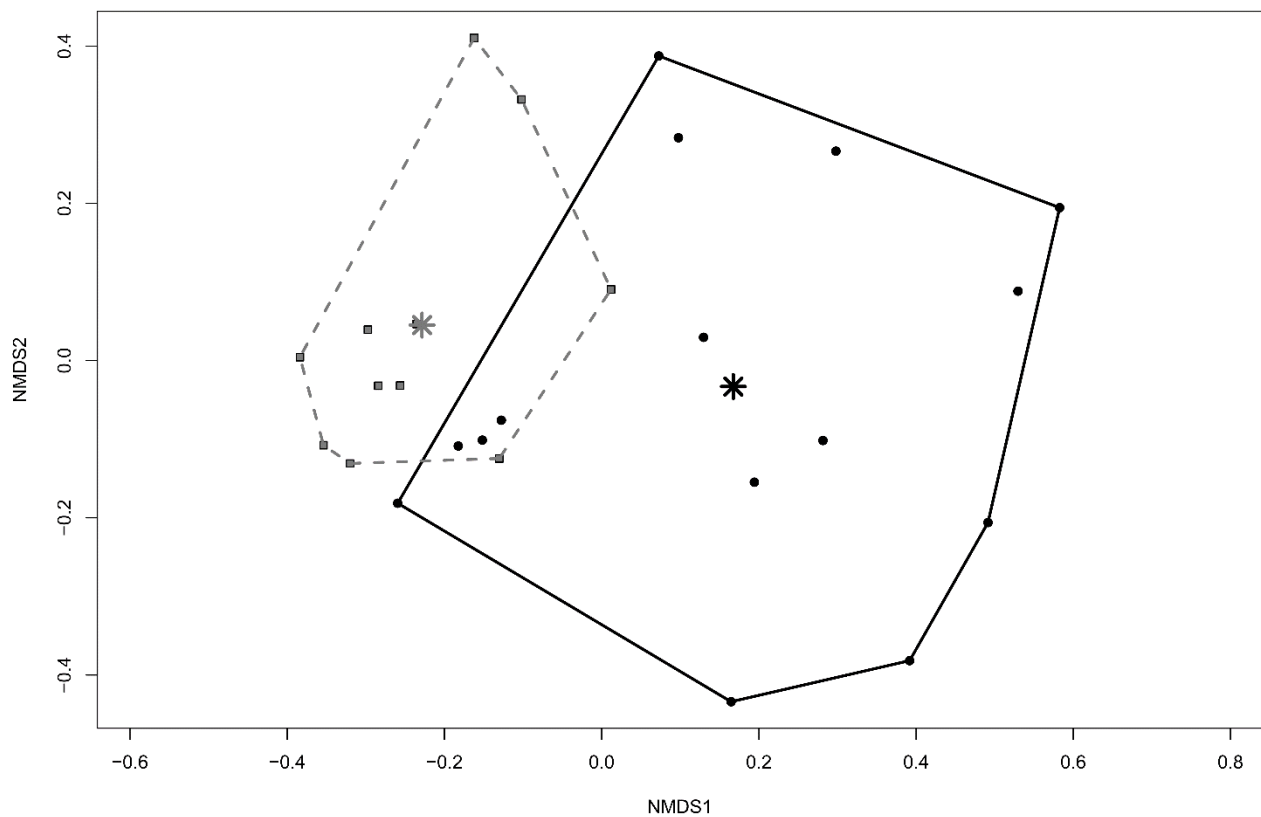


Figure S4: Non-metric Multi-Dimensional Scaling (NMDS) analysis of the diversity among gypsum endolithic samples from two differently coloured layers of colonization. Samples from the studied endolithic layers are enclosed within convex hulls with centroids marked by asterisks (black zone – black, full line, green zone – grey, dashed line). The analysis was based on Bray-Curtis distance matrix inferred from normalized abundances of the amplicon sequence variants (ASVs). The samples from black layers exhibited greater overall diversity.

Accession numbers

Colonizing gypsum under moderate climate: phototrophic endoliths and their pigments

Kateřina Němečková*, Jan Mareš, Lenka Procházková, Adam Culka, Filip Košek, Jacek Wierzechos, Linda Nedbalová, Jan Dudák, Veronika Tymlová, Jan Žemlička, Andreja Kust, Jan Zima Jr., Eva Nováková, and Jan Jehlička¹

* **Correspondence:** Corresponding Author: katerina.nemeckova@natur.cuni.cz

Cyanobacteria

SUB12910156 Seq1 OQ509403	SUB12910156 Seq16 OQ509418	SUB12910156 Seq31 OQ509433
SUB12910156 Seq2 OQ509404	SUB12910156 Seq17 OQ509419	SUB12910156 Seq32 OQ509434
SUB12910156 Seq3 OQ509405	SUB12910156 Seq18 OQ509420	SUB12910156 Seq33 OQ509435
SUB12910156 Seq4 OQ509406	SUB12910156 Seq19 OQ509421	SUB12910156 Seq34 OQ509436
SUB12910156 Seq5 OQ509407	SUB12910156 Seq20 OQ509422	SUB12910156 Seq35 OQ509437
SUB12910156 Seq6 OQ509408	SUB12910156 Seq21 OQ509423	SUB12910156 Seq36 OQ509438
SUB12910156 Seq7 OQ509409	SUB12910156 Seq22 OQ509424	SUB12910156 Seq37 OQ509439
SUB12910156 Seq8 OQ509410	SUB12910156 Seq23 OQ509425	SUB12910156 Seq38 OQ509440
SUB12910156 Seq9 OQ509411	SUB12910156 Seq24 OQ509426	SUB12910156 Seq39 OQ509441
SUB12910156 Seq10 OQ509412	SUB12910156 Seq25 OQ509427	SUB12910156 Seq40 OQ509442
SUB12910156 Seq11 OQ509413	SUB12910156 Seq26 OQ509428	SUB12910156 Seq41 OQ509443
SUB12910156 Seq12 OQ509414	SUB12910156 Seq27 OQ509429	SUB12910156 Seq42 OQ509444
SUB12910156 Seq13 OQ509415	SUB12910156 Seq28 OQ509430	SUB12910156 Seq43 OQ509445
SUB12910156 Seq14 OQ509416	SUB12910156 Seq29 OQ509431	SUB12910156 Seq44 OQ509446
SUB12910156 Seq15 OQ509417	SUB12910156 Seq30 OQ509432	SUB12910156 Seq45 OQ509447

SUB12910156 Seq46 OQ509448
 SUB12910156 Seq47 OQ509449
 SUB12910156 Seq48 OQ509450
 SUB12910156 Seq49 OQ509451
 SUB12910156 Seq50 OQ509452
 SUB12910156 Seq51 OQ509453
 SUB12910156 Seq52 OQ509454
 SUB12910156 Seq53 OQ509455
 SUB12910156 Seq54 OQ509456
 SUB12910156 Seq55 OQ509457
 SUB12910156 Seq56 OQ509458
 SUB12910156 Seq57 OQ509459
 SUB12910156 Seq58 OQ509460
 SUB12910156 Seq59 OQ509461
 SUB12910156 Seq60 OQ509462
 SUB12910156 Seq61 OQ509463
 SUB12910156 Seq62 OQ509464
 SUB12910156 Seq63 OQ509465
 SUB12910156 Seq64 OQ509466
 SUB12910156 Seq65 OQ509467
 SUB12910156 Seq66 OQ509468
 SUB12910156 Seq67 OQ509469
 SUB12910156 Seq68 OQ509470
 SUB12910156 Seq69 OQ509471
 SUB12910156 Seq70 OQ509472
 SUB12910156 Seq71 OQ509473
 SUB12910156 Seq72 OQ509474
 SUB12910156 Seq73 OQ509475

<https://submit.ncbi.nlm.nih.gov/subs/?search=SUB12910156>

Algae

OQ520113